Indian Journal of Pure & Applied Physics
Vol. 61, September 2023, pp. 759-761
DOI: 10.56042/ijpap.v61i9.3491

Synthetization and Characterization of Mo-doped Mn_4Si_7 by High Energy Ball Mill

Anjali Saini[a], R Gowrishankar[b], Mukesh Kumar Bairwa[a] & S Neeleshwar[a*]

[a]University School of Basic and Applied Sciences, Guru Gobind Singh Indraprastha University, Delhi 110 078, India

[b]Department of Physics, Sri Sathya Sai Institute of Higher Learning, Prasanthinilayam, A.P 515 134, India

Received 7 July 2023; accepted 11 August 2023

Mn_4Si_7 is a non-degenerating semiconductor with an indirect band gap of 0.77eV having multi-domain applications. The Mn_4Si_7 and Mo-doped Mn_4Si_7 were synthesized by high-energy ball milling at 600 RPM for 50H. From the X-ray diffraction (XRD), the tetragonal phase was observed. The average crystalline size was estimated by the Debye-Scherrer equation which lies below ~25 nm. The morphology studies reveal different shapes and sizes were observed by scanning electron microscopy (SEM).

Keywords: Phase purification; Ball milling; Manganese silicide; Earth-abundant; Doping

1 Introduction

Manganese silicide is an environment-friendly, earth-abundant, non-toxic material[1] and has many applications such as thermoelectric, lithium-ion batteries[2], electrical[3], photodiodes[4], optical[5], etc. Manganese silicides are known as Higher Manganese silicides (HMS) because it exists in different phases such as Mn_4Si_7, Mn_5Si_3, Mn_7Si_{12}, $Mn_{11}Si_{19}$, $Mn_{15}Si_{26}$, $Mn_{19}Si_{33}$, $Mn_{26}Si_{45}$, $Mn_{27}Si_{47}$, and $Mn_{39}Si_{68}$[1,6,7]. Among the HMS family, Mn_4Si_7 has non-degenerating semiconductor properties with an indirect band gap of 0.77 eV, while all other phases have degenerate semiconductors properties[8,9]. Mn_4Si_7 is a Nowotny chimney-ladder (NCL) tetragonal crystal structure that consists of manganese (Mn) atoms from chimney frame walls and silicon (Si) atoms from spiral ladders[9] (as shown in Fig. 1) and belongs to *P-4c2* space group with lattice parameters $a=b=$ 5.525 Å and $c=$ 17.463Å[10].

The challenge in the synthesization of single phase Mn_4Si_7 is the multiple phases formation of HMS. As per the literature survey, Mn_4Si_7 has been synthesized by different methods and different dopants (such as La[11], Ce[11], Cr[12], etc.) to understand their properties. One of the transport properties thermal conductivity (κ), which is very high for thermoelectric material. One needs to be optimized the κ, which may be selecting the suitable dopant at the Mn site. If the κ will be low, this system may be a good candidate for thermoelectric applications. In this paper, we doped Molybdenum (Mo) at the Mn site in Mn_4Si_7 to understand their transport mechanism, may be Mo-doping will reduce the lattice thermal conductivity by creating large mass fluctuations and lattice distortion owing to their size differences compared with the matrix element Mn. In this paper, we present the synthesization of the tetragonal phase of Mn_4Si_7 and Mo-doped Mn_4Si_7 at the Mn site by high energy ball milling technique, a simple, fast, scalable, and environmentally friendly.

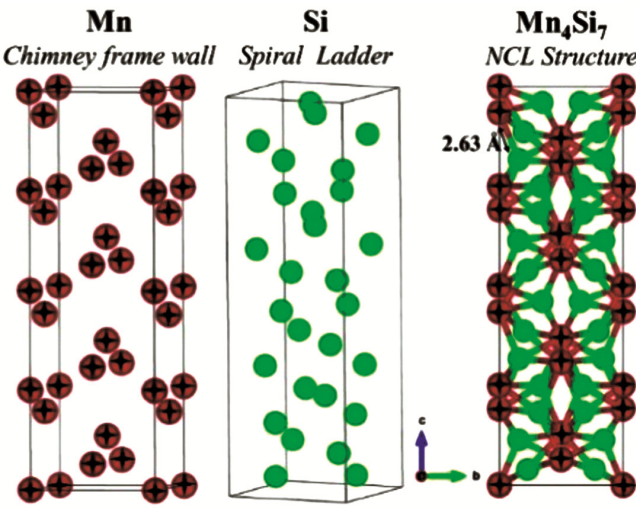

Fig. 1 — The Nowotny chimney-ladder tetragonal crystal structure of Mn_4Si_7 composed of Mn (chimney frame wall) atoms and superimposed Si (spiral ladder) atoms.

*Corresponding author: (E-mail: sn@ipu.ac.in)

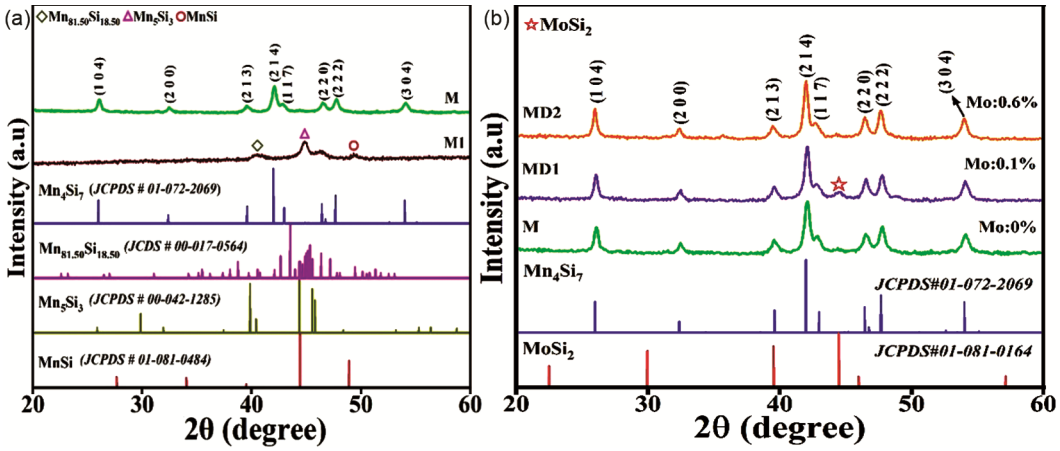

Fig. 2 — X-ray diffraction patterns of (a) the purely synthesized Mn_4Si_7 sample at 50H compared with standard data Mn_4Si_7 and (b) pure Mn_4Si_7 sample and Mo-doped Mn_4Si_7 samples compared with standard data of Mn_4Si_7 and $MoSi_2$. The peaks are well matched with Mn_4Si_7 (JCPDS # 01-072-2069) and $MoSi_2$ (JCPDS # 01-081-0164).

2 Experimental

The Mn_4Si_7 and Mo-doped (0.1% and 0.6%) Mn_4Si_7, were synthesized via high-energy ball milling at room temperature. The high-purity manganese pieces (99.9% Mn, Alfa Aesar), silicon lump (99.999% Si, Alfa Aesar), and molybdenum powder (99.9% Mo, Alfa Aesar), were homogenously mixed in a tungsten carbide jar and balls. Subsequently, the phase and crystallinity study were examined by X-ray diffraction (XRD) PANalytical X-pert diffractometer with Cu Kα-rays (λ = 1.54 Å). The morphology of samples was evaluated by scanning electron microscope (SEM, ZEISS EVO/18).

3 Results and Discussion

The environment-friendly and scalable, high-energy ball milling process was used to synthesize the pure phase of Mn_4Si_7 by optimizing various parameters such as RPM, milling time, on: off cycle and ball-to- powder weight ratio. Based on the phase diagram, Mn_4Si_7 was synthesize at RPM 500 for 50H (M1), but no desired phase was observed, as shown in Fig. 2 (a). After multiple trials, the pure phase of Mn_4Si_7 was successfully synthesized at RPM 600 for 50H in a tungsten carbide jar and balls. The clear view can observe in Fig. 2 (a) and compared with a standard database (JCPDS# 01-072-2069)[10] that only the Mn_4Si_7 phase was present, and no other phases were observed. After the successful synthesization of Mn_4Si_7, 0.1% Mo was doped at Mn-site in Mn_4Si_7 (synthesized at RPM 600 for 50H), as shown in Fig. 2 (b). Subsequently, increase the Mo-doping by 0.6% to eliminate the phase formation of $MoSi_2$, as shown in Fig. 2 (b). Fig. 2 (b) clearly show the polycrystalline nature of Mn_4Si_7 and Mo-doped Mn_4Si_7.

The crystalline size was estimated by Debye–Scherrer equation given:

$$D = \frac{k\lambda}{\beta cos\theta} \quad \ldots (1)$$

where k is Scherrer constant (k=0.9), λ the wavelength of the incident X-rays (1.5418 Å), θ the diffraction angle, and β stands for FWHM (full width at half maximum) for peaks. The average crystallite size for the Mn_4Si_7 sample was ~18 nm which increased to ~25 nm with 0.6% Mo-doped in the Mn_4Si_7 sample. The FWHM for the peak (2 1 4) was slightly reduce on Mo-doping, may indicates successful replacement of Mo at Mn site. From the XRD pattern, the lattice parameters *a* and *c* and unit cell volume *V* of Mn_4Si_7 and Mo-doped Mn_4Si_7 were calculated by the Bragg equation given:

$$n\lambda = 2d_{hkl}sin\theta \quad \ldots (2)$$

where n is the order of diffraction (usually n = 1), λ refers wavelength of X-ray diffraction, h, k, and l variables represents Miller-Bravais Indices of crystallographic plane, d_{hkl} stands for inter planar spacing. In the Mn_4Si_7 tetragonal structure, the plane spacing d is related to the lattice constants a = b ≠ c and the Miller indices by the following relation,

$$\frac{1}{d_{hkl}^2} = \frac{h^2+k^2}{a^2} + \frac{l^2}{c^2} \quad \ldots (3)$$

$$V = a^2c \quad \ldots (4)$$

The lattice parameters of Mn_4Si_7 a= 5.514 Å, c= 17.545 Å and unit cell volume was ~533 $Å^3$, which slightly increased on Mo doping 0.6% at the Mn site

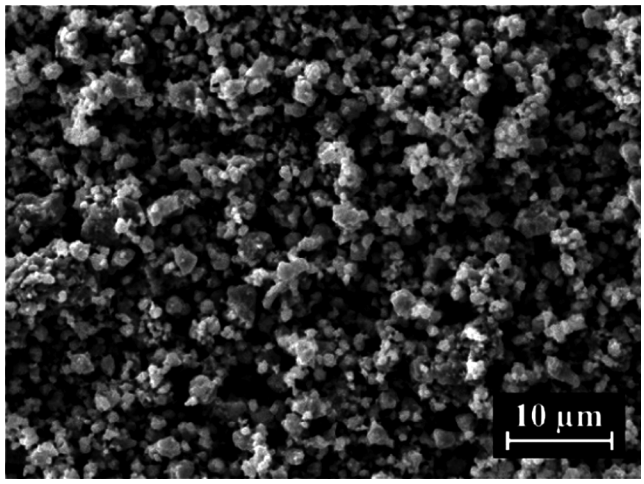

Fig. 3 — Secondary scattered SEM micrographs of Mn_4Si_7 sample synthesized via planetary ball milling thru WC vial and balls for 50H at 10 µm scale.

in Mn_4Si_7 a= 5.539 Å, c= 17.553 Å and unit cell volume was ~538 $Å^3$.The calculated values of lattice parameters and unit cell volume for synthesized samples, are in good agreement with the standard database. Indicates that both the samples were successfully synthesized and exhibited tetragonal phase formation for both the samples.

The high-energy ball milling technique is a scalable process that enables the synthesis of Mn_4Si_7. Fig. 3 shows the morphology of Mn_4Si_7 (M), indicating the presence of non-uniform particles of different shapes and sizes with random aggregation. The minimum and maximum average particle size was ~0.18 µm and ~6.83 µm, respectively.

4 Conclusion

The tetragonal phase of Mn_4Si_7 and Mo-doped Mn_4Si_7 was successfully synthesized by the high-energy ball milling technique. The Mo was systemically replaced by Mn-site, which affects the particle size by decreasing the FWHM, which results in the increment in the crystallite size from ~18 nm to ~25 nm. FWHM change may indicates successful replacement of Mo may at Mn-site. The lattice parameters and unit cell volume were slightly increased, on Mo-doping 0.6% from a= 5.514 Å, c= 17.545 Å and unit cell volume = ~533 $Å^3$ to a= 5.539 Å, c= 17.553 Å and unit cell volume= ~538 $Å^3$ and are in good agreement with the standard database. A non-uniform, different size and shape morphology was observed from scanning electron microscopy.

Acknowledgement

The authors are acknowledging the Central Research Instruments Facility of SSSIHL. SN acknowledge the FRGS (Grant No. GGSIPU/DRC/FRGS/2022/1223/13). Anjali Saini acknowledge the STRF (GGSIPU/ DRC/2021/675). Mukesh Kumar Bairwa acknowledge the IPRF (GGSIPU/DRC/2019/1453).

References

1 Rao S P, Saw A K, Chotia C, Okram G & Dayal V, *Appl Phys A*, 127 (2021) 621.
2 Li D, Wu Z Y, Yin Z W, Lu Y Q, Huang Z G, You J H, Li J T, Huang L & Sun S G, *Electrochimica Acta*, 260 (2018) 830.
3 André S, Gottlieb U, Affronte M & Laborde O, *J Magn Magn Mater*, 272 (2004) 519.
4 Shukurova D M, Orekhov A S, Sharipov B Z, Klechkovskaya V V & Kamilov T S, *Tech Phys*, 56 (2011) 1423.
5 Tarasov I A, Visotin M A, Kuznetzova T V, Aleksandrovsky A S, Solovyov L A, Kuzubov A A & Nikolaeva K M, *et al*., *J Mater Sci*, 53 (10) (2018) 7571.
6 Xi C, Weathers A, Carrete J, Mukhopadhyay S, Delaire O, Stewart D A, Mingo N, et al., *Nature Commun*, 6 (2015) 6723.
7 Neeleshwar S, Saini A, Bairwa M K, Bisht N, Katre A & Rao G N, In Nanomaterials for Innovative Energy Systems and Devices, *Singapore: Springer Nature Singapore*, (2022) 103.
8 Caprara S, Kulatov E & Tugushev V V, *The Eur Phys J B*, 85 (2012) 1.
9 Migas D B, Shaposhnikov V L, Filonov A B, Borisenko V E & Dorozhkin N N, *Phys Rev B*, 77 (2008) 075205.
10 Perumal, Suresh, Gorsse S, Ail U, Prakasam M, Rajasekar P & Umarji A M, *Mater Sci Semicond Process*, 104 (2019) 104649.
11 Li W, Zhang J M, He T, Wang K & Xie Q, *Mater Res Exp*, 6 (2019) 096309.
12 Shin D K, Ur S C, Jang K W & Kim I H, *J Electron Mater*, 43 (2014) 2104.